Characteristics of level-spacing statistics in chaotic graphene billiards

Liang Huang,[1,2,a)] Ying-Cheng Lai,[1,3,4] and Celso Grebogi[4]
[1]*School of Electrical, Computer and Energy Engineering, Arizona State University, Tempe, Arizona 85287, USA*
[2]*Institute of Computational Physics and Complex Systems, and Key Laboratory for Magnetism and Magnetic Materials of MOE, Lanzhou University, Lanzhou, Gansu 730000, China*
[3]*Department of Physics, Arizona State University, Tempe, Arizona 85287, USA*
[4]*Institute for Complex Systems and Mathematical Biology, School of Natural and Computing Sciences, King's College, University of Aberdeen, United Kingdom*

(Received 14 September 2010; accepted 20 December 2010; published online 2 March 2011)

A fundamental result in nonrelativistic quantum nonlinear dynamics is that the spectral statistics of quantum systems that possess no geometric symmetry, but whose classical dynamics are chaotic, are described by those of the Gaussian orthogonal ensemble (GOE) or the Gaussian unitary ensemble (GUE), in the presence or absence of time-reversal symmetry, respectively. For massless spin-half particles such as neutrinos in relativistic quantum mechanics in a chaotic billiard, the seminal work of Berry and Mondragon established the GUE nature of the level-spacing statistics, due to the combination of the chirality of Dirac particles and the confinement, which breaks the time-reversal symmetry. A question is whether the GOE or the GUE statistics can be observed in experimentally accessible, relativistic quantum systems. We demonstrate, using graphene confinements in which the quasiparticle motions are governed by the Dirac equation in the low-energy regime, that the level-spacing statistics are persistently those of GOE random matrices. We present extensive numerical evidence obtained from the tight-binding approach and a physical explanation for the GOE statistics. We also find that the presence of a weak magnetic field switches the statistics to those of GUE. For a strong magnetic field, Landau levels become influential, causing the level-spacing distribution to deviate markedly from the random-matrix predictions. Issues addressed also include the effects of a number of realistic factors on level-spacing statistics such as next nearest-neighbor interactions, different lattice orientations, enhanced hopping energy for atoms on the boundary, and staggered potential due to graphene-substrate interactions.
 [doi:10.1063/1.3537814]

In the last three decades, quantum nonlinear dynamics, an interdisciplinary field focusing on the quantum manifestations of classical chaos, has received a great deal of attention from a number of physics communities. Indeed, the quantization of chaotic Hamiltonian systems and signatures of classical chaos in quantum regimes are fundamental in physics and are directly relevant to fields such as condensed matter physics, atomic physics, nuclear physics, optics, and acoustics. Issues that have been pursued include energy-level statistics, statistical properties of wavefunctions, quantum chaotic scattering, electronic transport in quantum dots, localization, and the effect of magnetic field, etc. Existing works on quantum nonlinear dynamics are concerned almost exclusively with nonrelativistic quantum mechanical systems described by the Schrödinger equation, where the dependence of particle energy on momentum is quadratic. A natural question is whether phenomena in nonrelativistic quantum nonlinear dynamics can occur in relativistic quantum systems described by the Dirac equation, where the energy-momentum relation is linear. This paper focuses on the issue of energy level-spacing statistics by using chaotic graphene billiards whose hexagonal lattice structure generates a linear dependence of energy on wavevector about the Dirac points so that the motions of quasiparticles can be relativistic. We find that, for chaotic graphene billiards in the absence of magnetic field, the level-spacing distributions follow the statistics of random matrices from the Gaussian orthogonal ensemble (GOE). The GOE statistics are robust in that small perturbations from the ideal graphene billiard configuration such as high-order interactions in the tight-binding Hamiltonian, different lattice orientations, boundary bonds, and staggered potentials have little effect on the characteristics of the statistics. This result should be contrasted with the Gaussian unitary ensemble (GUE) statistics previously predicted for spin-half relativistic particles (e.g., neutrinos) in chaotic billiards. We have also investigated the effect of magnetic field on the level-spacing statistics and find that a weak magnetic field changes the GOE statistics to those of GUE, but a strong field can lead to large deviations from both the GOE and GUE statistics. Our results indicate that graphene systems can have properties that are not shared by either nonrelativistic quantum or purely relativistic quantum systems, and the distribution of energy levels may have implications to graphene-based devices that use quantum dots, a kind of "open" billiard structure.

[a)]Author to whom correspondence should be addressed. Electronic mail: liang.huang@asu.edu.

I. INTRODUCTION

A fundamental result in nonrelativistic quantum nonlinear dynamics is that, for systems whose classical dynamics are chaotic, their energy-level statistics are described by those of random matrices.[1–6] Particularly, if the system possesses the time-reversal symmetry, the energy level-spacings follow the distribution of those of random matrices from the Gaussian orthogonal ensemble (GOE). If, in addition to time-reversal symmetry, the particles have half-integer spin, the system will have the symplectic symmetry and, as a consequence, the resulted level-spacing statistics follow those of random matrices from the Gaussian symplectic ensemble (GSE). When the time-reversal symmetry is broken, e.g., as in the presence of a magnetic field, the level-spacing statistics are governed by the Gaussian unitary ensemble (GUE) random matrices. The transition from GOE to GUE statistics was first demonstrated in (Ref. 7). Both the GOE and GUE statistics were observed experimentally for nonrelativistic quantum (wave) systems exhibiting chaotic dynamics in the classical limit,[8–10] but so far there has been no experimental evidence for the GSE statistics.

In relativistic quantum mechanics, the seminal work of Berry and Mondragon[11] established that, for massless spin-half particles such as neutrinos[12] in a billiard, if the classical dynamics are integrable, the level-spacing statistics are Poissonian, which are similar to those in integrable nonrelativistic quantum systems. However, when the classical dynamics are chaotic, the level-spacing distributions are *persistently* those of GUE, even in the absence of any magnetic field. This is due to the chiral nature of Dirac particles and the confinement scalar potential, which break the time-reversal symmetry. Since its prediction over two decades ago,[11] this phenomenon has not been tested experimentally, partly due to the difficulty to construct relativistic quantum systems with chaotic classical dynamics in the laboratory.

Recently, graphene, a single, one-atom-thick sheet of carbon atoms arranged in a honeycomb lattice, has been realized in experiments.[13] In the low-energy regime, quasiparticle motions in graphene are characteristic of those of relativistic, massless Dirac fermions, and, consequently, devices made of graphene are potentially capable of operating at much higher speed than those based on the conventional silicon electronics.[14,15] Graphene confinements that have the geometric shape of chaotic billiards thus represent a potential experimental system for testing energy-level statistics in the relativistic quantum regime.

It thus seems quite feasible to test the prediction of Berry and Mondragon for the GUE statistics of Dirac particles by using classically chaotic graphene confinement systems. In this regard, a Poissonian type of level-spacing occurs for rectangular graphene dots. Increasing the strength of the disorder, i.e., edge roughness or defect concentration, tends to push the distribution toward that of GOE (Ref. 16). When the disorder concentration becomes higher, the distribution returns to Poissonian, due to the onset of Anderson localization.[17] In a recent Rapid Communication,[18] we find that, for "clean" chaotic graphene billiards, in the absence of magnetic field, the level-spacing statistics belong to the GOE universal class, in contrast to the GUE class predicted for relativistic Dirac particles. An intuitive explanation for this phenomenon is the following. In graphene, quasiparticles in the vicinity of a Dirac point obey the same Dirac equation as that for neutrino, but the confinement to realize the billiard plays a different role. Particularly, the abrupt edge termination in graphene billiard couples the two valleys in the momentum space. As a result, the wavefunctions for quasiparticles with wavevectors near the two Dirac points are no longer separable, rendering invalid description of the two-component spinor Dirac equation for the whole system. A full set of equations taking into account the two nonequivalent Dirac points and the boundary conditions are thus necessary to describe the motions of the relativistic particle. Especially, the time-reversal symmetry is preserved, suggesting that the system belong to either the GOE or the GSE class. In this regard, the abrupt edge termination in a graphene billiard can be described by a step function in the form of an infinite potential at the edge. Since the range of the potential is short, the two valleys in the momentum space are coupled, which also breaks the sublattice symmetry. Since both the pseudospin valley symmetry and the sublattice symmetry are broken, Kramer's degeneracy and consequently GSE statistics can be ruled out.[19] The resulting level-spacing statistics belong then to GOE. Similar effects have been noticed by Robnik and Berry that, in certain cases, although the system possesses neither time-reversal symmetry nor geometric symmetry (or other dynamical symmetries), it can be invariant under the combination of the two symmetries, and nontrivial representations can be found in which the Hamiltonian matrix elements are real, leading to GOE statistics (other than GUE) (Ref. 20).

A smooth mass term would preserve the valley symmetry but break the sublattice symmetry, which also breaks the time-reversal symmetry in each valley.[21] Since the two valleys are decoupled (no or weak intervalley scattering), the Hamiltonian consists of two degenerate blocks, each corresponding to a quasiparticle with unitary symmetry. However, the expected GUE level-spacing statistics have not been observed. This can be explained in that, although the mass term is relatively smooth, the system may still have some residual intervalley scattering, and the scattering time could be shorter than the relevant Heisenberg time scale for the level spacing, rendering the system to the GOE class.[21] These symmetry properties[22–25] are also related to pseudospin effects in the system, which could lead to absence of backscattering[26,27] and weak-localization or antilocalization phenomena,[19,28–32] and also to universal conductance fluctuations of different universal classes.[21,33]

In this paper, we present results from a detailed study of the level-spacing statistics in chaotic graphene billiards, taking into full account quantum-mechanical symmetry considerations. Particularly, we shall focus on two types of billiards without any geometric symmetries but whose classical dynamics are fully chaotic. In order to generate a large number of energy levels for reliable statistics, we use relatively large sizes, in which the confinements contain tens of thousands of atoms. Utilizing the tight-binding framework, we obtain strong evidence for GOE statistics in such billiards

in the absence of magnetic field. To address the question of whether the GOE statistics are stable and thus potentially experimentally observable in graphene devices, we use more realistic tight-binding models to incorporate factors such as next nearest-neighbor coupling, different lattice orientations, enhanced hopping energy of the boundary atoms, and staggered potential due to graphene-substrate interaction. Our results indicate that, although these considerations may cause changes in the band structure such as the induction of a band gap, a shift in the Dirac point, or modification in the details of the band structure, the linear energy-momentum relation is preserved. As a result, the spacing statistics for the levels around the Dirac points are *persistently* of the GOE class.

We also study systematically the effect of an external magnetic field on level-spacing statistics in chaotic graphene billiards. In the presence of a weak magnetic field, the time-reversal symmetry of the system is broken and GUE statistics arise, as for chaotic billiards in the nonrelativistic quantum regime. As the magnetic field becomes stronger, Landau levels set in. The sublevels within the Landau levels are degenerate so that they have zero spacing. Excluding these degenerate sublevels, we find signatures of the GOE statistics. This is, however, not related to time-reversal symmetry, but rather an artificial effect caused by Landau levels. For energy levels far from the Dirac points, the electronic densities of state are high, and the effect of Landau levels is suppressed; therefore, the level-spacing statistics belong to the GUE class.

In Sec. II, we introduce the tight-binding Hamiltonian based method to calculate the energy levels for large graphene billiards. In Sec. III, we present theory and numerical results for GOE statistics for quasiparticles near the Dirac points, taking into account a number of realistic physical factors. In Sec. IV, we describe the level-spacing statistics in the presence of weak and strong magnetic fields. Conclusions and discussions are given in Sec. V.

II. TIGHT-BINDING METHOD FOR CALCULATING ENERGY LEVELS IN GRAPHENE BILLIARDS

For a graphene confinement in the presence of a magnetic field, the tight-binding Hamiltonian is given by

$$\hat{H} = \sum (-t_{ij})|i\rangle\langle j|, \tag{1}$$

where the summation is over all pairs of nearest neighboring atoms, and

$$t_{ij} = t\exp(-i\frac{2\pi}{\phi_0}\int_{\mathbf{r}_j}^{\mathbf{r}_i} d\mathbf{r}\cdot\mathbf{A}) \tag{2}$$

is the nearest-neighbor hopping energy, $\mathbf{A}$ is the vector potential associated with the magnetic field, $\phi_0 = h/e = 4.136 \times 10^{-15}$ Tm^2 is the magnetic flux quantum, and $t \approx 2.8$ eV is the nearest-neighbor hopping energy in the absence of magnetic field.[34] Using the Landau gauge, the vector potential is given by $\mathbf{A} = (-By, 0, 0)$ for a perpendicular uniform magnetic field B pointing out of the billiard plane. For convenience, we shall use the magnetic flux $\phi = BS$ through a hexagonal plaque as a parameter characterizing the strength of the magnetic field, where the area is $S = 3\sqrt{3}/2a_0^2 = 5.24$ Å^2, and $a_0 = 1.42$ Å is the atom separation in the graphene lattice. The onsite energy has been neglected as we assume it is the same for all carbon atoms in the confinement. The eigenenergies can be calculated by diagonalizing the tight-binding Hamiltonian.

Our focus will be on the energy spectrum around the Dirac points to address the relativistic quantum nature of the quasiparticle motions in graphene. Figure 1 shows the energy-wavevector relation for an infinite graphene lattice in the absence of magnetic field. As can be seen from the contour lines around each Dirac point, when the energy is low, say, $E/t = 0.2$, the contour line is almost circle, indicating that the $E-\mathbf{k}$ relation is isotropic, which is characteristic of the relativistic Dirac equation. For larger energy, say $E/t = 0.6$, trigonal warping distortions occur,[35] leading to an anisotropic $E-\mathbf{k}$ relation bearing the hexagonal symmetry of graphene lattice. The distortions become more dominant as the energy is increased further. We shall then concentrate on energy levels in the low energy range $0 < E/t < 0.4$ so that our results can be meaningfully compared with those from the relativistic neutrino billiards.

Figure 2 shows the band structure for a zigzag nanoribbon without or with a magnetic field. For a sufficiently strong magnetic field, the linear $E-\mathbf{k}$ relation, even for small energy, is violated, as Fig. 2(d) shows. To observe the transition from GOE to GUE statistics under a magnetic field in the relativistic quantum regime, we restrict our study to the regime where the linear $E-\mathbf{k}$ relation is preserved while the magnetic field is strong enough so that the GUE statistics emerge even for nonrelativistic quantum chaotic billiards. We shall then study three cases: $\phi = 0$ (without magnetic field), $\phi = 1/8000\phi_0$ (weak magnetic field), and $\phi = 1/800\phi_0$ (strong magnetic field).[36]

We study two billiard shapes that are commonly used in the study of level-spacing statistics, the Africa billiard[7] and

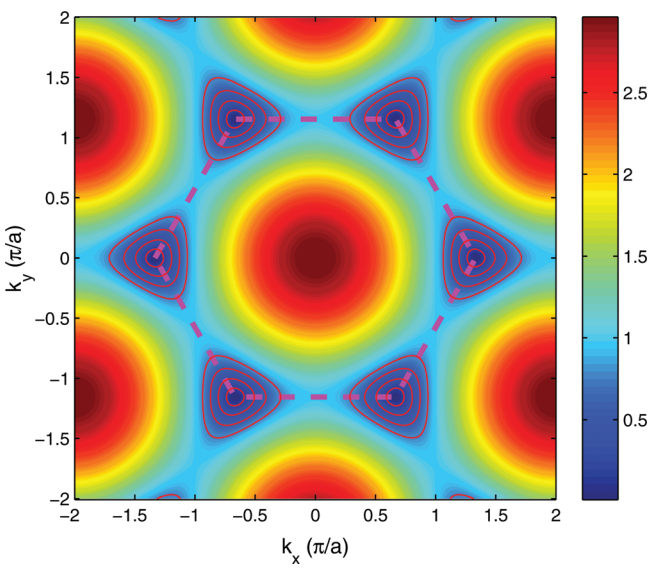

FIG. 1. (Color online) Contour plot of energy in the momentum space for an infinite graphene flake, where $a = \sqrt{3}\,a_0 = 2.46$ Å is the lattice constant along the zigzag direction. The dashed line indicates the first Brillouin zone. The four sets of solid contour lines around each individual Dirac points are for $E/t = 0.2, 0.4, 0.6, 0.8$ (inside out), respectively.

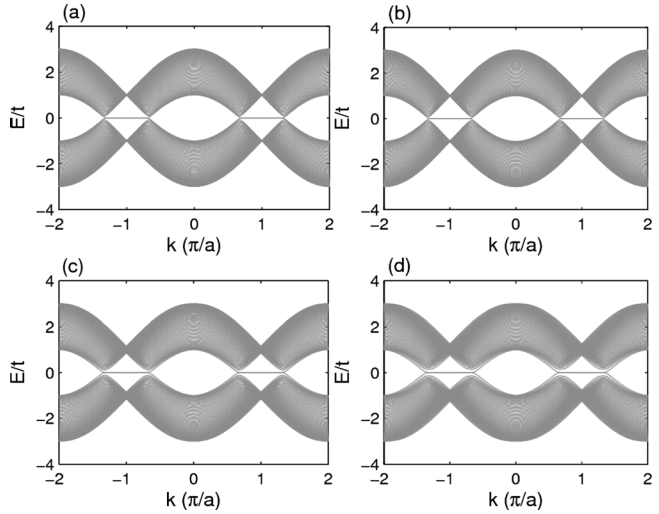

FIG. 2. Energy-momentum relation for graphene nanoribbon with zigzag horizontal boundary: (a) $\phi = 0$; (b) $\phi = 1/8000\phi_0$; (c) $\phi = 1/800\phi_0$; and (d) $\phi = 1/500\phi_0$. Each layer of the ribbon contains 100 atoms.

one-eighth of the Sinai billiard, as shown in Fig. 3. We use MATLAB to calculate the eigenvalues. The number of atoms contained in a billiard is about 35 000, which represents the limit set by the memory of our computer (60 GB). The area of each billiard is about 950 nm^2, and the number of levels in the energy range $0 < E/t < 0.4$ is about 550. When we calculate the local density-of-state (LDS) patterns, we employ a smaller size, typically containing about 10 000 atoms, as it requires more memory to calculate the eigenvectors. In the cases of studying realistic effects without magnetic field, we use a larger size of about 42 000 atoms, as solving eigenvalues of real symmetric matrices needs less memory than that when solving complex Hermitian matrices.

III. LEVEL-SPACING STATISTICS OF CHAOTIC GRAPHENE BILLIARDS IN THE ABSENCE OF MAGNETIC FIELD

For nonrelativistic chaotic quantum billiard, the smoothed wavevector staircase function for positive eigenvalues is given by[37]

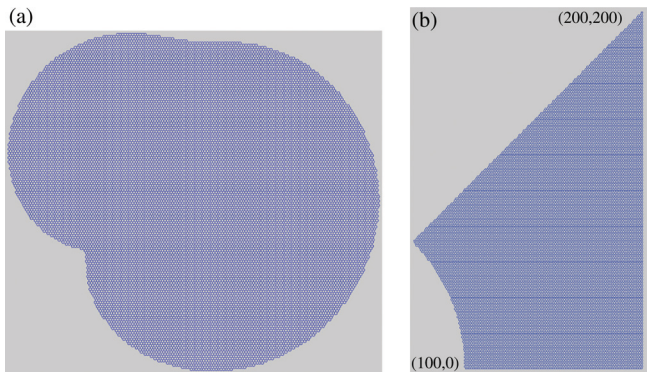

FIG. 3. (Color online) Chaotic graphene billiards. (a) Africa billiard of 35542 atoms. The outline is determined by the equation $x + iy = 64(z + 02z^2 + 0.2z^3\ e^{i\pi/3})a$, where z is the unit circle in the complex plane, $a = \sqrt{3}a_0 = 2.46$ Å. The area of the billiard is $A = 934$ nm^2. (b) One-eighth of the Sinai billiard with 37401 atoms. The coordinates are in units of lattice constant a. The area is $A = 1.607 \times 10^4\ a^2 = 972$ nm^2.

$$\langle N(k)\rangle = Ak^2/4\pi + \gamma Lk/4\pi + \ldots, \tag{3}$$

where A is the area of the billiard, L is its parameter, and $\gamma = 1$ (or -1) for Neumann (or Dirichlet) boundary conditions. For relativistic spin-half particles such as the neutrino, Berry and Mondragon found that the same formula holds except that $\gamma = 0$ (Ref. 11)

$$\langle N(k)\rangle = Ak^2/4\pi + C_1 + \ldots, \tag{4}$$

where $C_1 = -1/12$ is a constant.

For our chaotic graphene billiard, around a Dirac point, we have $E = \hbar v_F k$, where $v_F = \sqrt{3}ta/2\hbar$ is the Fermi velocity, and $a = 2.46$ Å is the lattice constant. Thus, $E = \sqrt{3}tak/2$. For the nth energy-level E_n, we have

$$k_n = \frac{2}{\sqrt{3}a} \cdot \frac{E_n}{t}.$$

Once the eigenenergy E_n is determined, the corresponding wavevector k_n can be obtained through the above relation. For the graphene billiard shown in Fig. 3(a), Fig. 4(a) shows, for eigenenergies in the range $0 < E_n/t < 0.4$, the wavevector staircase function. The solid curve is given by

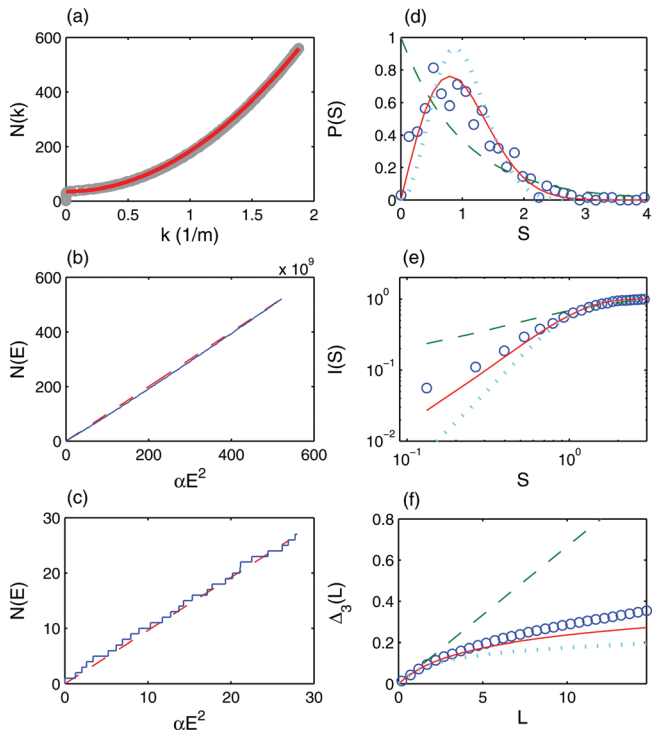

FIG. 4. (Color online) Level-spacing statistics for the Africa billiard in Fig. 3(a) in the absence of magnetic field ($\phi = 0$). (a) Wavevector staircase function $N(k)$ for eigenenergies $0 < E_n/t < 0.4$, where the number of energy levels is 560 (circles). The curve is $\langle N(k)\rangle = Ak^2/(2\pi) + 35$ [Eq. (5)]. (b) Spectral staircase function $N(E)$ vs αE^2, for $0.02 < E_n/t < 0.4$ with 522 levels, where α is the unfolding normalization constant. The dashed straight line is the averaged staircase function [Eq. (6)]. (c) Magnification of part of (b) for $0.02 < E_n/t < 0.1$ with 28 levels. (d) Unfolded level-spacing distribution $P(S)$. (e) Cumulative unfolded level-spacing distribution $I(S)$. (f) Spectral rigidity Δ_3. In (d)–(f), numerical data are represented by open circles and the lines are theoretical predictions from the random-matrix theory: dashed line for Poissonian, solid line for GOE, and dotted line for GUE statistics. The same legend holds for subsequent figures in this paper.

$$\langle N(k)\rangle = Ak^2/2\pi + C_1', \tag{5}$$

where $C_1' = 35$ is a fitting constant. Equation (5) differs from Eq. (4) in the leading "Weyl" term by a factor of 2. This can be understood as follows. For a single Dirac point, one expects $\langle N(k)\rangle$ to follow Eq. (4). However, a finite graphene has two nonequivalent Dirac points; thus, $\langle N(k)\rangle$ should be twice of that given by Eq. (4), so the denominator becomes 2π (instead of 4π). The fitting constant C_1' is due to the edge states on the segments of the zigzag boundaries of the graphene billiard where their energies are all about zero. For zigzag ribbon the edge states exist for $E < E_c = \hbar v_F/L = \sqrt{3}ta/(2L)$, where L is the width of the ribbon.[38] The sizes of our graphene billiards are about $100a$, leading to $E_c \simeq 0.01t$. Figure 5 shows two typical edge states and a normal state. The edge states are localized on segments of the zigzag boundaries. These states are essentially degenerate states, contributing to an artificial bias in the spectral staircase function for small energy values. Therefore, we set a minimum value $2E_c = 0.02t$ for E_n to exclude the edge states from consideration.

Because we have $E = \hbar v_F k$ for graphene billiards, the smoothed spectral staircase function is given by

$$\langle N(E)\rangle = \frac{AE^2}{2\pi\hbar^2 v_F^2} + C_2 = \alpha E^2 + C_2, \tag{6}$$

where $\alpha = A/(2\pi\hbar^2 v_F^2)$ is the unfolding normalization parameter and C_2 is now zero after setting $2E_c$ as the minimum value of E_n. Figure 4(b) shows the spectral staircase function of E_n for $0.02 < E_n/t < 0.4$, and Fig. 4(c) shows a magnification of part of Fig. 4(b) for eigenenergies in the range $0.02 < E/t < 0.1$. The dashed lines in these two panels are Eq. (6) with $C_2 = 0$. They agree well with the numerical results.

Now define $x_n \equiv \langle N(E_n)\rangle$ as the unfolded spectra. Let $S_n = x_{n+1} - x_n$ be the nearest-neighbor spacing and $P(S)$ be the distribution function of S_n. It can be verified that $\int SP(S)dS = 1$. For nonrelativistic quantum billiards, the distribution of this unfolded level-spacing follows several universal classes, depending on the nature of the corresponding classical dynamics and symmetry. Particularly, if the system is classically integrable, the distribution is Poissonian[39]

$$P(S) = e^{-S}. \tag{7}$$

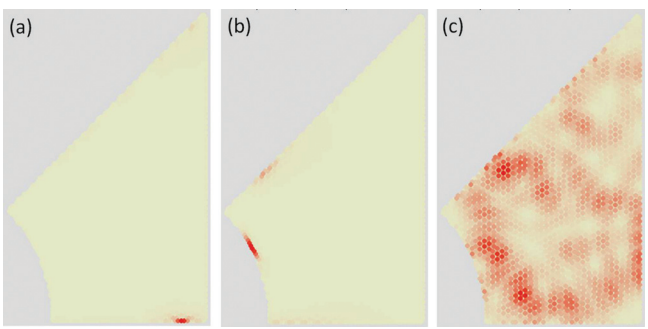

FIG. 5. (Color online) Typical edge states (a), (b) and a normal state (c) for one-eighth of the Sinai billiard with $N = 9230$ atoms. The energy values are $E_n/t = 1.610 \times 10^{-14}$, 7.475×10^{-6}, 0.313 for (a–c), respectively.

For quantum billiards that are completely chaotic in the classical limit and do not possess any geometric symmetry,[40,41] the level-spacing distributions follow the GOE statistics if the system has time-reversal symmetry[42]

$$P(S) = \frac{\pi}{2} S e^{-\pi S^2/4}, \tag{8}$$

and GUE statistics if the system has no time-reversal symmetry

$$P(S) = \frac{32}{\pi^2} S^2 e^{-(4/\pi)S^2}. \tag{9}$$

The cumulative level-spacing distribution can then be obtained by

$$I(S) = \int_0^S P(S')\mathrm{d}S'. \tag{10}$$

The distribution of the unfolded level-spacing for the Africa graphene billiard is shown in Fig. 4(d), and the cumulative distribution is shown in Fig. 4(e). From the figures, we see that the level-spacing follows the GOE statistics.

To obtain further evidence for the GOE statistics, we calculate the spectral rigidity $\Delta_3(L)$ for the graphene billiards, which is used to measure long-range spectral fluctuations and is defined as[43]

$$\Delta_3(L) = \left\langle \min(a,b)L^{-1} \int_{-L/2}^{L/2} dx\{N(x_0+x) - ax - b\}^2 \right\rangle, \tag{11}$$

where the average is over x_0. Numerically, if n unfolded levels $\tilde{x}_i = x_i - x_0$ lie in the interval $[-L, L]$, e.g., $-L \le \tilde{x}_1 \le \cdots \le \tilde{x}_n \le L$, performing the integral in the above equation yields[44]

$$\begin{aligned}\Delta_3(2L, x_0) = {} & \frac{n^2}{16} - \frac{1}{4L^2}\left[\sum_{i=1}^{n} \tilde{x}_i\right]^2 \\ & + \frac{3n}{8L^2}\left[\sum_{i=1}^{n} \tilde{x}_i^2\right] - \frac{3}{16L^4}\left[\sum_{i=1}^{n} \tilde{x}_i^2\right]^2 \\ & + \frac{1}{2L}\left[\sum_{i=1}^{n} (n-2i+1)\tilde{x}_i\right],\end{aligned} \tag{12}$$

and $\Delta_3(L) = \langle \Delta_3(L, x_0)\rangle_{x_0}$. Theoretically, $\Delta_3(L)$ for a correlated unfolded energy-level sequence is given by

$$\Delta_3(L) = \frac{1}{15L^4}\left[L^5 - \int_0^L du(L-u)^3(2L^2 - 9Lu - 3u^2)Y(u)\right], \tag{13}$$

where $Y(u)$ is the following two-level cluster function:[45]

$$\begin{aligned} Y(u) &= 0 \qquad \text{for Poisson} \\ Y(u) &= U(u)^2 + \frac{d}{du}U(u) \times \int_u^\infty dt U(t) \quad \text{for GOE}, \\ Y(u) &= U(u)^2 \qquad \text{for GUE}, \end{aligned}$$

and $U(u) = \sin(\pi u)/(\pi u)$.

Figure 4(f) shows the spectral rigidity for the calculated eigenenergies of the Africa billiard. This, together with Figs. 4(d) and 4(e), represents strong evidence that the level-spacing distribution in a chaotic graphene billiard in the relativistic quantum regime follows the GOE statistics. Figure 6 plots the same quantities as Fig. 4 for the one-eighth of Sinai billiard in Fig. 3(b). Figures 6(a)–6(c) verify Eqs. (5) and (6), and Figs. 6(d)–6(f) show unequivocally the GOE nature in the level-spacing statistics. Comparing Fig. 6 with Fig. 4, we notice that the level-spacing statistics from the 1/8 Sinai billiard are closer to the theoretical expectation of GOE. However, a careful examination of systems of different sizes reveals that the discrepancy between the two billiards is not caused by the difference in shapes, but by the number of levels used in the statistics, or the size of the system. The larger the system is, the closer the statistics to the theoretical expectation.

The GOE statistics of unfolded level-spacing seem to be counterintuitive as one would expect that the graphene chaotic billiards should exhibit the same GUE level-spacing distribution as the neutrino billiard,[11] because they obey the same massless Dirac equation. However, as explained in Sec. I, because the graphene has two nonequivalent Dirac points (valleys), the time-reversal symmetry for the neutrino is actually the symplectic symmetry for graphene, which is the time-reversal symmetry in a single valley.[25] Thus, the time-reversal symmetry breaking caused by the chirality in the neutrino billiards does not infer time-reversal symmetry breaking in graphene billiards. As a matter of fact, the time-reversal symmetry of graphene, taking into account of both valleys, is preserved in the absence of a magnetic field,[25] which explains the GOE level-spacing statistics.

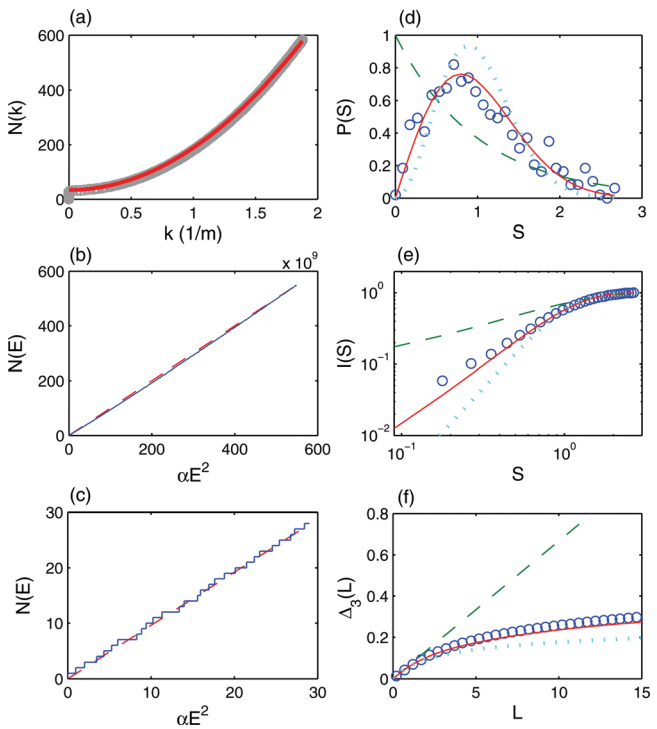

FIG. 6. (Color online) Level-spacing statistics for the graphene billiard in Fig. 3(b) in the absence of magnetic field ($\phi = 0$). (a) Wavevector staircase function $N(k)$ for eigenenergies $0 < E_n/t < 0.4$ for a total of 582 energy levels. The curve is $\langle N(k)\rangle = Ak^2/(2\pi) + 34$ [Eq. (4)]. (b) Spectral staircase function $N(E)$ vs $\propto E^2$ for calculated eigenenergies E_n (solid curve). The dashed straight line is the averaged staircase function [Eq. (6)]. The energy range is $0.02 < E_n/t < 0.4$ and the number of levels is 549. The constant C_2 is zero since the edge states are excluded. (c) A magnification of part of (b) for $0.02 < E_n/t < 0.1$ with 29 levels. (d) Unfolded level-spacing distribution $P(S)$. (e) Cumulative unfolded level-spacing distribution $I(S)$. (f) Spectral rigidity Δ_3.

The results so far are for ideal chaotic graphene billiards. In experimental situations, a number of nonidealities can arise, such as interactions beyond the nearest neighbors, lattice orientation, substrate properties, etc. To be experimentally observable, the GOE statistics should be robust even when these nonidealities are present. It is thus important to investigate the robustness of the level-spacing statistics of chaotic graphene billiards under various realistic considerations.

A. Effect of next nearest-neighbor coupling

In the absence of magnetic field, the tight-binding Hamiltonian incorporating the next nearest-neighbor interactions is given by

$$\hat{H} = \sum_{t} (-t)|i\rangle\langle j| + \sum_{t'} (-t')|i\rangle\langle j|, \tag{14}$$

where the first summation is over all pairs of nearest neighboring atoms, and the second summation is over all pairs of next nearest neighboring atoms with coupling strength $t' = 0.1t$ (Ref. 34). In this case, around the Dirac point $\mathbf{K}$, letting $\mathbf{k} = \mathbf{K} + \mathbf{q}$, to the first order in $|\mathbf{q}|$ the energy is given by

$$E_{\pm} \approx 3t' \pm v_F \hbar |\mathbf{q}|. \tag{15}$$

Thus, the linear energy-momentum relation persists except with a shift in energy of $3t'$ at the Dirac points. Figures 7(b) and 7(d) plot the band structure of a zigzag ribbon taking into account the next nearest-neighbor couplings. For comparison, the corresponding cases of $t' = 0$ are shown in Figs. 7(a) and 7(c). In addition to the shift in the energy, another feature can be seen. Particularly, for $t' = 0$, the positive energy band connecting the two Dirac points is flat, i.e., $E/t \sim 0$, which contributes to the edge states for $E/t \gtrsim 0$. However, for $t' = 0.1t$, the band bends downward. Thus, if we consider the energies above the Dirac points, e.g., $0.3 < E_n/t < 0.7$, there is no edge-state contributions.

The level-spacing statistics are shown in Fig. 8 for eigenenergies in the range of $0.3 < E_n/t < 0.7$ with about 700 levels. We observe the GOE statistics. Thus, although the next nearest-neighbor interactions modify the band structure and consequently may have implications in realistic applications,[46] they have little effect on the level-spacing statistics.

B. Effect of lattice orientation

So far we have assumed that the horizontal direction of the graphene billiards is zigzaged. Since the energy-momentum relation (especially the location of the Dirac points) is direction-dependent, and the billiard shape has no geometric symmetry, it is worthwhile to examine whether the lattice orientation

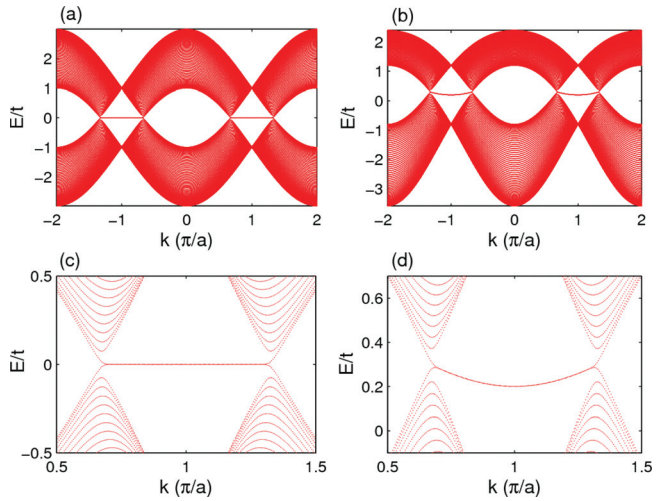

FIG. 7. (Color online) Band structure of a zigzag graphene ribbon having 120 atoms in a vertical layer: (a), (c) $t' = 0$ (without next nearest-neighbor coupling); (b), (d) $t' = 0.1t$ (next nearest-neighbor interactions included). Lower panels are the respective magnifications of upper panels around the Dirac point.

of the graphene billiard will affect the level-spacing statistics. To do so, we first generate a rectangular graphene flake, rotate it with angle θ, and then form the confinement by cutting off the outside atoms. Again, boundary atoms with only one bond are removed to avoid artificial scattering effects. We have done calculations for the Africa billiard for $\theta = \pi/7$ and $\theta = \pi/2$ (chosen arbitrarily), and the results for $\theta = \pi/7$ are shown in Fig. 9. We can see that, although the details of the distribution are somewhat different from those of the $\theta = 0$ case (Fig. 4), the GOE statistics are well preserved. Comparing the three cases (i.e., $\theta = 0, \pi/7, \pi/2$), we find that the main difference is the number of edge states, as for different orientations the numbers of zigzag terminations are different. Figure 10 shows the eigenenergies right above the

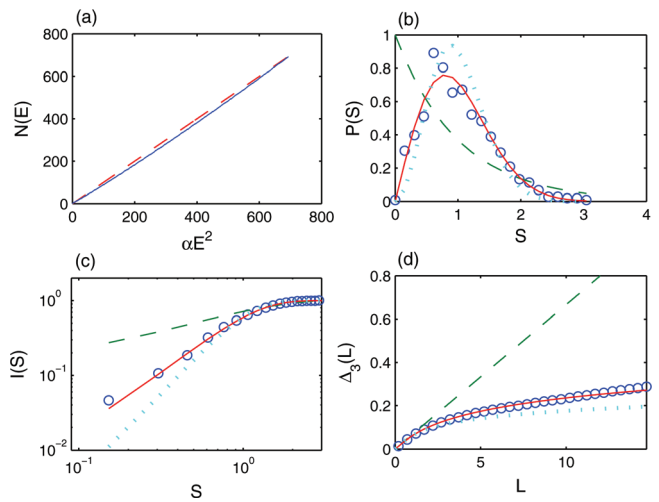

FIG. 8. (Color online) In the presence of next nearest-neighbor interactions, level-spacing statistics for the Africa billiard of $N = 42505$ atoms in the absence of magnetic field. (a) Spectral staircase function $N(E)$ vs αE^2 for $0.3(=3t') < E_n/t < 0.7$ (solid curve), where the origin of E has shifted to $3t'$. The dashed straight line is the averaged staircase function [Eq. (6)]. (b) Unfolded level-spacing distribution $P(S)$. (c) Cumulative unfolded level-spacing distribution $I(S)$. (d) Spectral rigidity Δ_3.

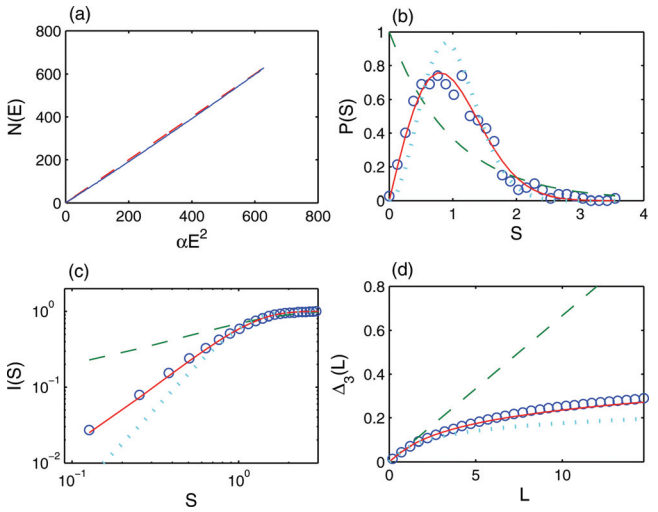

FIG. 9. (Color online) In the presence of lattice tilting (see text), level-spacing statistics for the Africa billiard of $N = 42518$ atoms. The angle of lattice tilting is $\theta = \pi/7$ and there is no magnetic field. (a) Spectral staircase function $N(E)$ vs $\alpha\ E^2$ for $0.02 < E_n/t < 0.4$ (solid curve). The dashed straight line is the averaged staircase function [Eq. (6)]. (b) Unfolded level-spacing distribution $P(S)$. (c) Cumulative unfolded level-spacing distribution $I(S)$. (d) Spectral rigidity Δ_3.

Dirac point for the three orientations. It can be seen that the $\theta = 0$ case has more edge states. The edge states are, however, excluded in the level-spacing statistics. For different orientations, the values of the eigenenergies are different, as shown in Fig. 10. In addition, the details of the wavefunction concentrations associated with various eigenenergies are also different. However, our calculations reveal that the level-spacing statistics belong to the same GOE class, indicating the robustness of the GOE statistics for chaotic graphene billiards in the relativistic quantum regime.

C. Effect of boundary bonds and staggered potentials

We have assumed uniform hopping energy throughout the billiard. However, the bonds associated with the boundary atoms can be shorter. As a result, the hopping energy of the boundary atoms can be, e.g., 10% larger than that associated with the inner atoms. This edge effect is in fact crucial

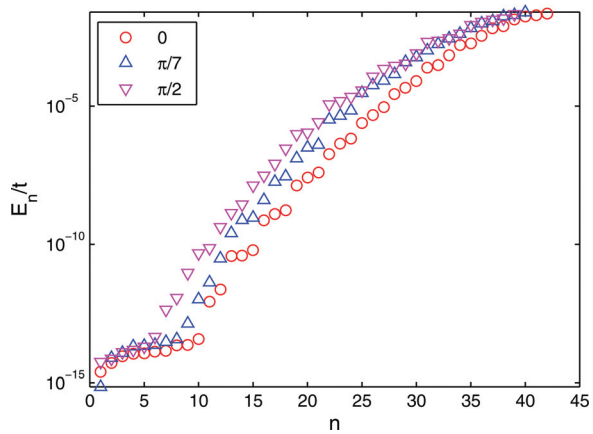

FIG. 10. (Color online) Eigenenergies close to the Dirac point for the three orientations $(\theta = 0, \pi/7, \pi/2)$ for the African billiard with $N = 42505$, 42518, 42512 atoms, respectively.

for determining the values and scaling rule for the band gap of graphene armchair or zigzag ribbons.[47] We have examined its effect on the level-spacing statistics. Specifically, after generating the billiard, we determined the boundary atoms, and changed the hopping energy of these atoms with other atoms inside the billiard to $1.1t$. Our computations revealed no observable difference in the level-spacing statistics.

Another important feature is staggered potential, that is, the two inequivalent sublattices are biased to different potentials, which can be a natural way to tune the band gap of graphene nanoribbon as the staggered potential can arise naturally from the interaction between graphene and the substrate.[48,49] Figure 11 shows the energy gap caused by a staggered potential $U_0 = 0.1t$. The edge states are visible as the horizontal line segment at $E_n = \pm\ U_0$. The level-spacing statistics for the energy levels in the range $U_0 + 2E_c = 0.12 < E_n/t < 0.5$ are shown in Fig. 12. The statistics apparently still belong to the GOE class.

IV. EFFECT OF MAGNETIC FIELD ON LEVEL-SPACING STATISTICS

A. Weak magnetic field

The presence of a magnetic field breaks the time-reversal symmetry of the graphene system[25] and, consequently, the level-spacing distribution belongs to the GUE class. Figure 13 plots the same quantities as Fig. 4 for the same Africa billiard with a uniform magnetic field $\phi = \phi_0/8000$. Figure 14 presents the level-spacing statistics for the one-eighth Sinai billiard in Fig. 3(b) with $\phi = \phi_0/8000$. Figures 13(a)–13(c) and 14(a)–14(c) indicate that the level statistics agree well with the semiclassical predictions [Eqs. (5) and (6)]. The unfolded level-spacing statistics are shown in Figs. 13(d)–13(f) and 14(d)–14(f). In both cases, we observe strong signatures of GUE statistics.

B. Strong magnetic field

For a stronger magnetic field, e.g., for $\phi = \phi_0/800$, the quantization of the energy levels to Landau levels becomes

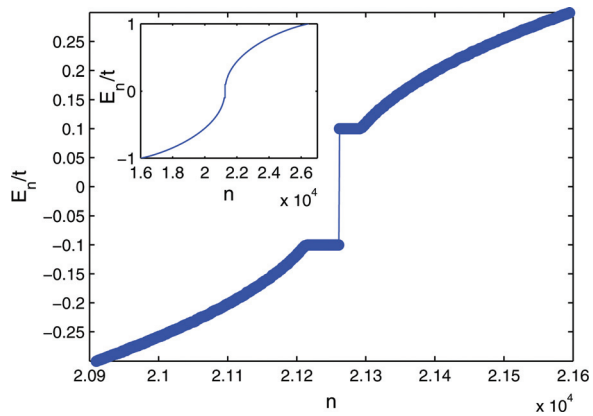

FIG. 11. (Color online) Eigenenergies of the Africa billiard of $N = 42505$ atoms with staggered potential $U_0 = 0.1t$, which demonstrates the band gap caused by the staggered potential.

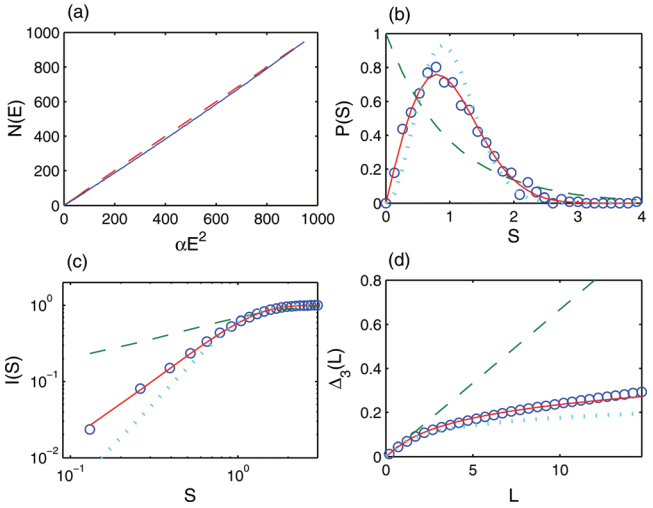

FIG. 12. (Color online) Level-spacing statistics for the Africa billiard of $N = 42505$ atoms with staggered potential $U_0 = 0.1t$ in the absence of magnetic field. (a) Spectral staircase function $N(E)$ vs αE^2 (solid curve). The dashed straight line is the averaged staircase function [Eq. (6)]. The eigenenergies are in the range $U_0 + 2E_c = 0.12 < E_n/t < 0.5$ that contains 946 levels. (b) Unfolded level-spacing distribution $P(S)$. (c) Cumulative unfolded level-spacing distribution $I(S)$. (d) Spectral rigidity Δ_3.

important. The energy levels are clustered, leading to $\partial N/\partial E \to \infty$, appeared in the plots of staircase function [Figs. 15(a)–15(c) and 16(a)–16(c)] as the large vertical steps. The staircase counting function deviates markedly

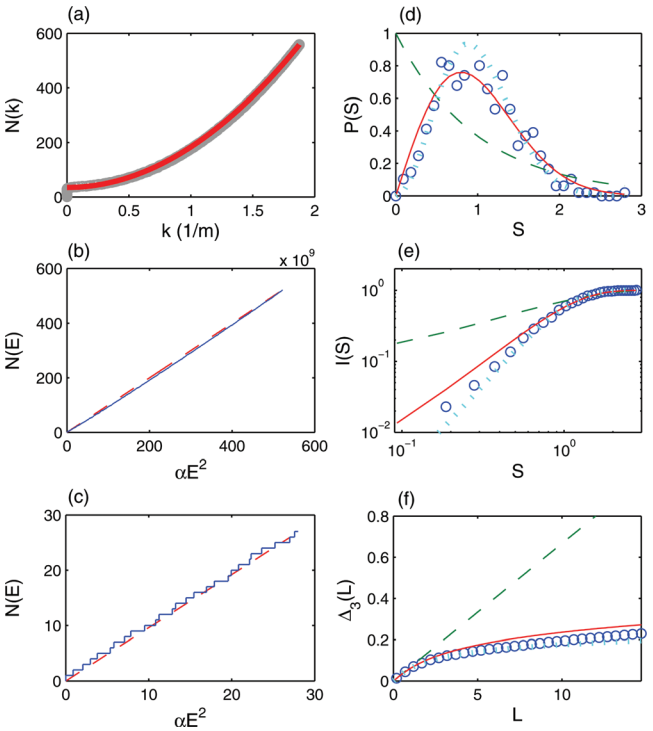

FIG. 13. (Color online) Level-spacing statistics for the Africa billiard in Fig. 3(a) for $\phi = \phi_0/8000$. (a) Wavevector staircase function $N(k)$ for eigenenergies $0 < E_n/t < 0.4$ with a total of 559 energy levels. The curve is $\langle N(k)\rangle = Ak^2/(2\pi) + 35$ [Eq. (4)]. (b) Spectral staircase function $N(E)$ vs αE^2 for $0.02 < E_n/t < 0.4$ (solid curve). There are 522 levels. The dashed straight line is the averaged staircase function [Eq. (6)]. (c) Magnification of part of (b) for $0.02 < E_n/t < 0.1$ with 28 levels. (d) Unfolded level-spacing distribution $P(S)$. (e) Cumulative unfolded level-spacing distribution $I(S)$. (f) Spectral rigidity Δ_3.

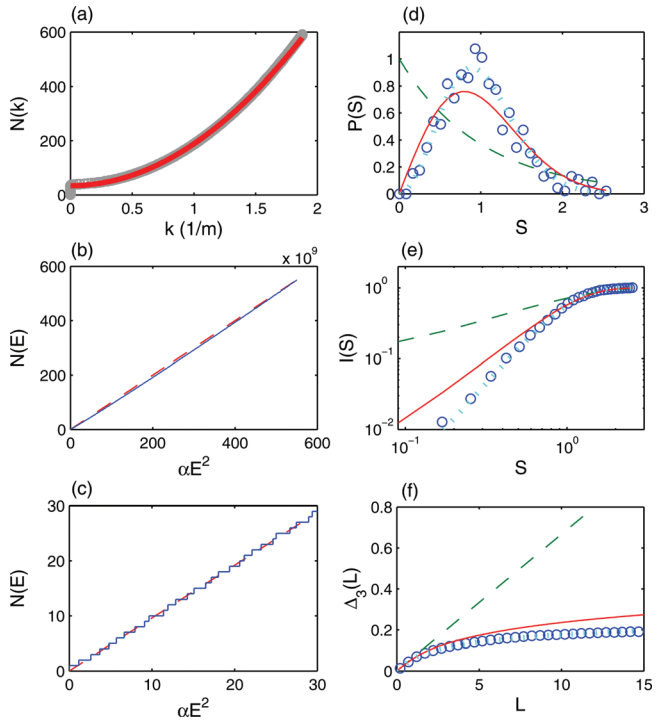

FIG. 14. (Color online) Level-spacing statistics for one-eighth of the Sinai billiard in Fig. 3(b) for $\phi = \phi_0/8000$. (a) Wavevector staircase function $N(k)$ for eigenenergies $0 < E_n/t < 0.4$ with a total of 590 energy levels. The curve is $\langle N(k)\rangle = Ak^2/(2\pi) + 34$ [Eq. (4)]. (b) Spectral staircase function $N(E)$ vs αE^2 for $0.02 < E_n/t < 0.4$ (solid curve). There are 550 levels. The dashed straight line is the averaged staircase function [Eq. (6)]. (c) Magnification of a part of (b) for $0.02 < E_n/t < 0.1$ with 30 levels. (d) Unfolded level-spacing distribution $P(S)$. (e) Cumulative unfolded level-spacing distribution $I(S)$. (f) Spectral rigidity Δ_3.

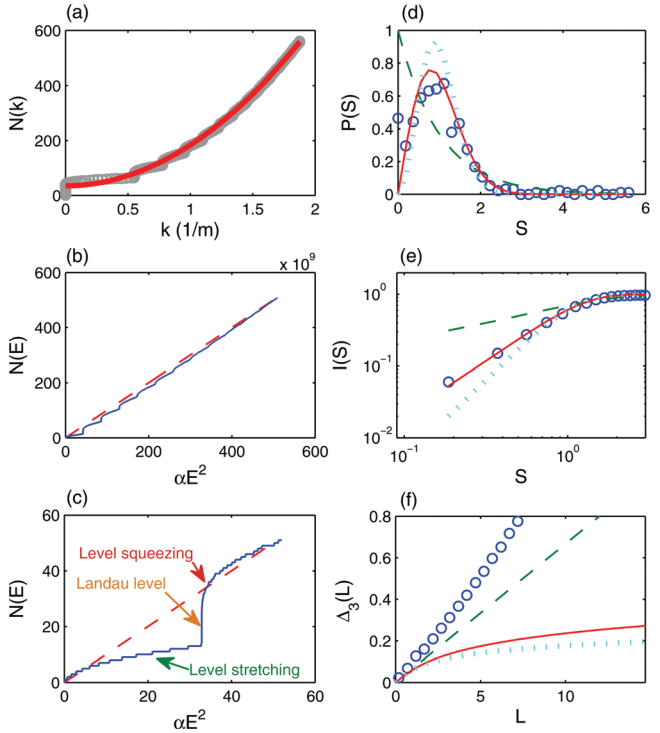

FIG. 15. (Color online) Level-spacing statistics for the Africa billiard in Fig. 3(a) for $\phi = \phi_0/800$. (a) Wavevector staircase function $N(k)$ for eigenenergies $0 < E_n\ t < 0.4$ with a total of 560 energy levels. The curve is $\langle N(k)\rangle = Ak^2/(2\pi) + 34$ [Eq. (4)]. (b) Spectral staircase function $N(E)$ vs αE^2 for $0.02 < E_n/t < 0.4$ (solid curve). There are 509 levels. The dashed straight line is the averaged staircase function [Eq. (6)]. (c) Magnification of part of (b) for $0.02 < E_n/t < 0.15$ with 52 levels. (d) Unfolded level-spacing distribution P/S). (e) Cumulative unfolded level-spacing distribution $I(S)$. (f) Spectral rigidity Δ_3.

from the semiclassical predictions. The unfolded level-spacing distribution is shown in Figs. 15(d) and 16(d). The high value of first data point is originated from the spacing of energy levels within the Landau levels, which is basically zero compared to the normal level-spacings. Figures 15(e) and 16(e) show the cumulative distribution excluding the first point. The results show deviations from GUE and are in fact closer to GOE. Intuitively, this can be understood by noting that the Landau levels "squeeze" the energy levels around them [Figs. 15(c) and 16(c)], resulting in smaller level-spacings and larger values of $P(S)$ for small S. At the same time, because the overall slope of the staircase counting function is unchanged, the squeezing of energy levels around the Landau levels tends to stretch the energy levels in between the different Landau levels [Figs. 15(c) and 16(c)], yielding large level-spacings and larger values of $P(S)$ for large S. This stretching "pushes" the level-spacing distribution from GUE to GOE. Similar results have been observed in nonrelativistic quantum chaotic billiards where the system is described by Schrödinger equation, in the energy range where the density of states is low and the Landau levels are apparent.

Figures 15(f) and 16(f) show the spectral rigidity, which does not fall into any of the three known categories. This is because the staircase function no longer follows the semiclassical prediction when the effects of the Landau levels cannot be neglected for strong magnetic field.

To illustrate the effect of level stretching and level squeezing as caused by the eigenstates entering and leaving a Landau level, respectively, we plot the eigenstates around a Landau level in Fig. 17. A general observation is that, when the energy is increased to enter a Landau level, both the pattern and eigenenergies vary significantly, with less correlation between adjacent states. When the energy is increased further to leave the Landau level, the consecutive states show a systematic variation and the level-spacing becomes smaller. Note that, for extremely strong magnetic field, almost all the energy levels are quantized to Landau levels, between two Landau levels the states are such that the electrons/holes are localized at the edge of the billiard, as in nonrelativistic two-dimensional electron gas systems.[50]

For higher energy levels where the Landau level is not apparent, the level-spacing statistics return to the GUE class again. Figure 18 shows, for the one-eighth Sinai billiard, the level-spacing statistics for eigenenergies in the range $0.4 < E/t < 0.7$. Figures 18(b)–18(d) indicate GUE statistics. Although in this energy range trigonal warping becomes dominant (Fig. 1), which renders the theoretical description of Dirac equation inappropriate, the energy levels can be accessible in experiments and thus relevant to graphene quantum-dot operations. We note that $N(E_n)$ still depends hyperbolically on E_n [Fig. 18(a)], indicating a linear dependence between E_n and k_n. This can be understood that in this energy range, the trigonal warping determines the scars

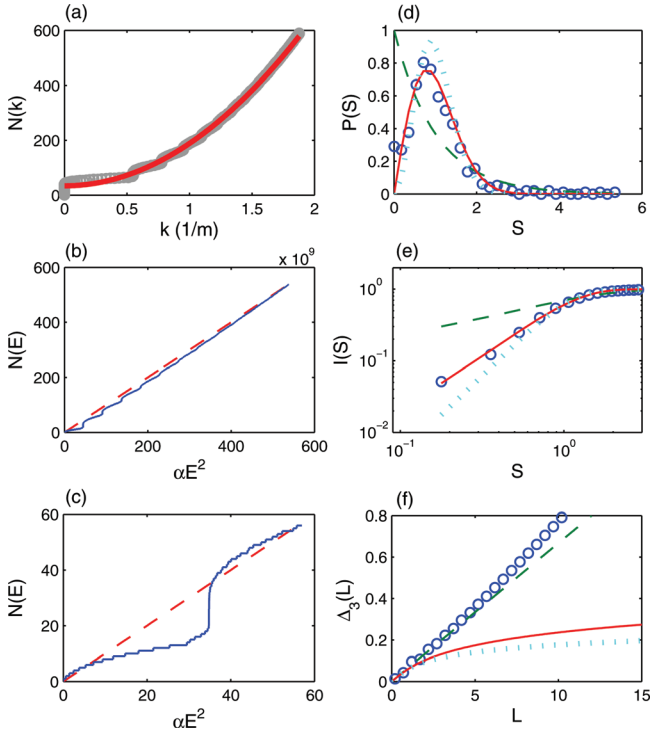

FIG. 16. (Color online) Level-spacing statistics for one-eighth of the Sinai billiard in Fig. 3(b) for $\phi = \phi_0/800$. (a) Wavevector staircase function $N(k)$ for eigenenergies $0 < E_n/t < 0.4$ with a total of 589 energy levels. The curve is $\langle N(k)\rangle = Ak^2/(2\pi) + 34$ [Eq. (4)]. (b) Spectral staircase function $N(E)$ vs αE^2 for $0.02 < E_n/t < 0.4$ (solid curve). There are 538 levels. The dashed straight line is the averaged staircase function [Eq. (6)]. (c) Magnification of a part of (b) for $0.02 < E_n/t < 0.1$ with 57 levels. (d) Unfolded level-spacing distribution $P(S)$. (e) Cumulative unfolded level-spacing distribution $I(S)$. (f) Spectral rigidity Δ_3.

(electron density patterns obtained from eigenstates) in the system, and restrains them to having line segments only in three directions, e.g., from the Dirac points to the origin.[51] Along these directions, the $E-k$ relation is approximately linear up to $E/t \sim 1$. This explains the hyperbolic relation between $N(E_n)$ and E_n even for high energies far away from the Dirac point.

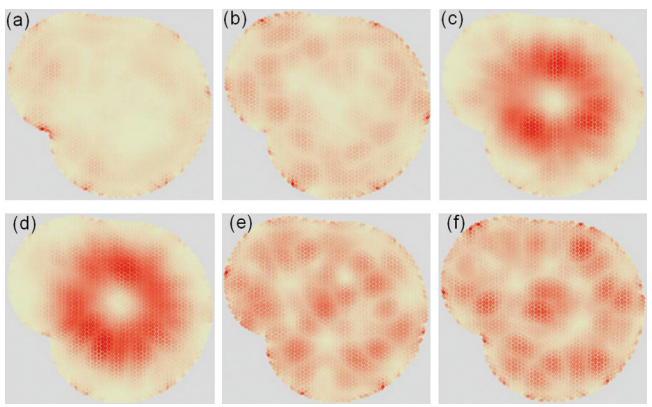

FIG. 17. (Color online) Some typical consecutive states for the Africa billiard around a Landau level for a smaller system with 13 859 atoms. The energies are $E/t = 0.1596, 0.1651, 0.1664, 0.1666, 0.1684, 0.1693$ for (a)–(f), respectively. The level-spacings for these states are $\Delta E/t = 0.0055, 0.0013, 0.0002, 0.0018, 0.0009$. (c) and (d) are two Landau-level states.

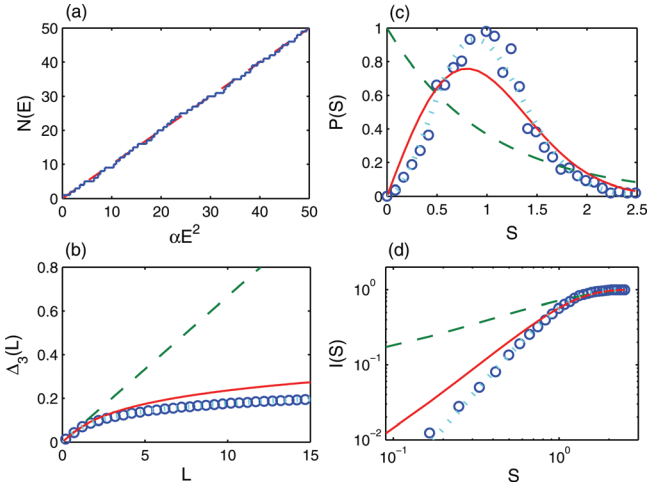

FIG. 18. (Color online) Level-spacing statistics for the billiard in Fig. 3(b) for $\phi = \phi_0/800$. (a) Spectral staircase function $N(E)$ vs αE^2 for $E_n/t > 0.4$ (solid curve). The dashed straight line is the averaged staircase function [Eq. (6)]. (b) Spectral rigidity Δ_3. (c) Unfolded level-spacing distribution $P(S)$. (d) Cumulative unfolded level-spacing distribution $I(S)$. (b)–(d) are for energy levels in the range of $0.4 < E_n/t < 0.7$ with a total of 1294 levels.

The above observation of the GUE statistics for higher eigenenergies, from another aspect, corroborates our arguments that, around the Dirac point, the energy level-spacing statistics are shifted "artificially" to GOE by the Landau levels. This could be important as the level-spacing can possibly be revealed in the peak spacings of the conductance in the corresponding quantum dots made from "open" billiards.[52]

Magnetic field effects in classical billiards have been studied in Ref. 53, where it was found that for billiards with sufficiently smooth boundaries, such as the integrable elliptical billiard system, flyaway chaos can be induced by an intermediate magnetic field, but increasing the magnetic field further to the Landau regime can squeeze out the existence of this chaos.

V. CONCLUSIONS

We have examined the level-spacing statistics of chaotic graphene billiards in the low-energy regime around the Dirac point where the energy-momentum relation is linear so that the quasiparticles are characteristic of relativistic motion. Our general finding is that, in the absence of magnetic field, the level-spacings follow the GOE statistics. The GOE distribution is robust with respect to various modifications to the Hamiltonian such as the addition of next nearest-neighbor interactions, different lattice orientations, boundary-bond effect, and staggered potentials. This should be contrasted to the GUE statistics predicted for relativistic, spin-half particles such as neutrinos in chaotic billiards in the absence of magnetic field. The underlying mechanism for the GOE statistics in chaotic graphene billiards is the finite-boundary induced coupling of the quasiparticle motions about the two Dirac points, which preserves the time-reversal symmetry.

We have also investigated the effect of magnetic field on the level-spacing statistics, which breaks the time-reversal symmetry. For weak magnetic field, the level-spacing statistics become of the GUE type. However, for strong magnetic

field, around the Dirac point where the density of states is low, Landau levels arise. As a result, energy levels are squeezed about and stretched in between the Landau levels, shifting the level-spacing distribution from GUE to GOE. This is, however, an artificial effect because, in this case, the spectral staircase function, one of the fundamental quantities in characterizing energy-level statistics, deviates significantly from the semiclassical prediction. For higher energy levels well above the Dirac point for which the relativistic quantum description becomes less relevant, the GUE statistics are recovered in the presence of a magnetic field.

In this paper, we have focused on the chaotic graphene billiards. Mixed billiards exhibiting regular motion on invariant tori for some initial conditions and chaotic motion for the complementary initial conditions are also important subjects in quantum chaos,[54] and the level-spacing statistics of mixed graphene billiards deserve future investigation.

ACKNOWLEDGMENTS

L.H. and Y.C.L. were supported by AFOSR under Grant No. F9550-09-1-0260 and by ONR under Grant No. N0014-08-1-0627. C.G. was supported by BBSRC under Grants No. BB-F00513X and No. BB-G010722. L.H. was also supported by NSFC under Grant No. 11005053.

[1]G. Bohigas and M.-J. Giannoni, in *Mathematical and Computational Methods in Nuclear Physics*, Lecture Notes in Physics, Vol. 209 (Springer, Berlin, 1984); G. Bohigas, M.-J. Giannoni, and C. Schmit, Phys. Rev. Lett. **52**, 1 (1984).
[2]M. V. Berry, Proc. R. Soc. London, Ser. A **400**, 229 (1985).
[3]M. Gutzwiller, *Chaos in Classical and Quantum Mechanics* (Springer, Berlin, 1990).
[4]F. Haake, *Quantum Signatures of Chaos*, 2nd ed. (Springer, Berlin, 2001).
[5]H. A. Weidenmüller and G. E. Mitchell, Rev. Mod. Phys. **81**, 539 (2009).
[6]A requirement for the applicability of random-matrix theory is that the system possess no geometric symmetry.
[7]M. V. Berry and M. Robnik, J. Phys. A **19**, 649 (1986).
[8]H. J. Stöckmann, *Quantum Chaos: An Introduction* (Cambridge University Press, Cambridge, England, 1999).
[9]U. Stoffregen, J. Stein, H.-J. Stöckmann, M. Kuś, and F. Haake, Phys. Rev. Lett. **74**, 2666 (1995).
[10]P. So, S. M. Anlage, E. Ott, and R. N. Oerter, Phys. Rev. Lett. **74**, 2662 (1995).
[11]M. V. Berry and R. J. Mondragon, Proc. R. Soc. London, Ser. A **412**, 53 (1987).
[12]Neutrinos have a minuscule, but nonzero mass. See G. Karagiorgi, A. Aguilar-Arevalo, J. M. Conrad, M. H. Shaevitz, K. Whisnant, M. Sorel, and V. Barger, Phys. Rev. D **75**, 013011 (2007).
[13]K. S. Novoselov, A. K. Geim, S. V. Morozov, D. Jiang, Y. Zhang, S. V. Dubonos, I. V. Grigorieva, and A. A. Firsov, Science **306**, 666 (2004).
[14]F. Miao, S. Wijeratne, Y. Zhang, U. C. Coskun, W. Bao, and C. N. Lau, Science **317**, 1530 (2007).
[15]L. A. Ponomarenko, F. Schedin, M. I. Katsnelson, R. Yang, E. W. Hill, K. S. Novoselov, and A. K. Geim, Science **320**, 356 (2008).
[16]F. Libisch, C. Stampfer, and J. Burgdörfer, Phys. Rev. B **79**, 115423 (2009).
[17]I. Amanatidis and S. N. Evangelou, Phys. Rev. B **79**, 205420 (2009).
[18]L. Huang, Y.-C. Lai, and C. Grebogi, Phys. Rev. E **81**, 055203(R) (2010).
[19]H. Suzuura and T. Ando, Phys. Rev. Lett. **89**, 266603 (2002).
[20]M. Robnik, and M. V. Berry, J. Phys. A **19**, 669 (1986); M. Robnik, in *Quantum Chaos and Statistical Nuclear Physics*, Lecture Notes in Physics, Vol. 263 (Springer-Verlag, Berlin, 1986).
[21]J. Wurm, A Rycerz, I. Adagideli, M. Wimmer, K. Richter, and H. U. Baranger, Phys. Rev. Lett. **102**, 056806 (2009).
[22]S. Ryu, C. Mudry, H. Obuse, and A. Furusaki, Phys. Rev. Lett. **99**, 116601 (2007).
[23]K. Nomura, M. Koshino, and S. Ryu, Phys. Rev. Lett. **99**, 146806 (2007).
[24]P. M. Ostrovsky, I. V. Gornyi, and A. D. Mirlin, Phys. Rev. Lett. **98**, 256801 (2007).
[25]C. W. J. Beenakker, Rev. Mod. Phys. **80**, 1337 (2008).
[26]C. Bena, Phys. Rev. Lett. **100**, 076601 (2008).
[27]I. Brihuega, P. Mallet, C. Bena, S. Bose, C. Michaelis, L. Vitali, F. Varchon, L. Magaud, K. Kern, and J. Y. Veuillen, Phys. Rev. Lett. **101**, 206802 (2008).
[28]T. Ando, T. Nakanishi, and R. Saito, J. Phys. Soc. Jpn. **67**, 2857 (1998).
[29]S. V. Morozov, K. S. Novoselov, M. I. Katsnelson, F. Schedin, L. A. Ponomarenko, D. Jiang, and A. K. Geim, Phys. Rev. Lett. **97**, 016801 (2006).
[30]E. McCann, K. Kechedzhi, V. I. Falko, H. Suzuura, T. Ando, and B. L. Altshuler, Phys. Rev. Lett. **97**, 146805 (2006).
[31]A. F. Morpurgo and F. Guinea, Phys. Rev. Lett. **97**, 196804 (2006).
[32]X. Wu, X. Li, Z. Song, C. Berger, and W. A. de Heer, Phys. Rev. Lett. **98**, 136801 (2007).
[33]M. Y. Kharitonov and K. B. Efetov, Phys. Rev. B **78**, 033404 (2008).
[34]A. H. Castro Neto, F. Guinea, N. M. R. Peres, K. S. Novoselov, and A. K. Geim, Rev. Mod. Phys. **81**, 109 (2009).
[35]R. Saito, G. Dresselhaus, and M. S. Dresselhaus, Phys. Rev. B **61**, 2981 (2000); A. Rycerz, J. TworzydŁo, and C. W. J. Beenakker, Nat. Phys. **3**, 172 (2007); V. V. Cheianov, V. Fal'ko, and B. L. Altshuler, Science **315**, 1252 (2007); J. L. Garcia-Pomar, A. Cortijo, and M. Nieto-Vesperinas, Phys. Rev. Lett. **100**, 236801 (2008).
[36]The magnetic field can be scaled down for larger confinements to yield similar effects.
[37]H. P. Baltes and E. R. Hilf, *Spectra of Finite Systems* (B.-I. Wissenschaftseverlag, Mannheim, 1976).
[38]L. Brey and H. A. Fertig, Phys. Rev. B **73**, 235411 (2006).
[39]M. V. Berry and M. Tabor, Proc. R. Soc. London **356**, 375 (1977).
[40]M. L. Mehta, *Random Matrices* (Academic, New York, 1967).
[41]A. Bohr and B. R. Mottelson, *Nuclear Structure*, Vol. 1 (Benjamin, New York, 1969), Appendix 2C, pp. 294–301.
[42]Here we do not consider GSE since it is irrelevant to our studies.
[43]F. J. Dyson and M. L. Mehta, J. Math. Phys. **4**, 701 (1963).
[44]O. Bohigas and M. J. Giannoni, Ann. Phys. **89**, 393 (1975).
[45]B. Liu, G.-C. Zhang, L. Ding, J.-H. Dai, and H.-J. Zhang, Phys. Lett. A **260**, 406 (1999).
[46]A. R. Wright, F. Liu and C. Zhang, Nanotechnology **20**, 405203 (2009).
[47]Y.-W. Son, M. L. Cohen, and S. G. Louie, Phys. Rev. Lett. **97**, 216803 (2006).
[48]C. L. Kane and E. J. Mele, Phys. Rev. Lett. **95**, 146802 (2005).
[49]S. Y. Zhou, G.-H. Gweon, A. V. Fedorov, P. N. First, W. A. de Heer, D.-H. Lee, F. Guinea, A. H. Castro Neto, and A. Lanzara, Nature Mater. **6**, 770 (2007).
[50]A. H. MacDonald, Phys. Rev. B **29**, 6563 (1984).
[51]L. Huang, Y.-C. Lai, D. K. Ferry, S. M. Goodnick, and R. Akis, Phys. Rev. Lett. **103**, 054101 (2009).
[52]Y. Alhassid and C. H. Lewenkopf, Phys. Rev. Lett. **75**, 3922 (1995).
[53]M. Robnik and M. V. Berry, J. Phys. A **18**, 1361 (1985); M. Robnik, in *Nonlinear Phenomena and Chaos*, Malvern Physics Series (Adam-Hilger, Bristol, 1986); J. Phys. A **19**, 3619 (1986).
[54]M. Robnik, Nonlinear Phenom. Complex Syst. (Minsk) **1**, 1 (1998); B. Batistić and M. Robnik, J. Phys. A: Math. Theor. **43**, 215101 (2010).